PHYSICAL REVIEW B **77**, 195417 (2008)

Density-functional investigation of metal-silicon cage clusters $M\mathrm{Si}_n$ (M=Sc, Ti, V, Cr, Mn, Fe, Co, Ni, Cu, Zn; n=8–16)

Ling-ju Guo,[1] Gao-feng Zhao,[1,*] Yu-zong Gu,[2] Xia Liu,[1] and Zhi Zeng[3]
[1]*School of Physics and Electronics, Henan University, Kaifeng 475004, People's Republic of China*
[2]*Institute of Microsystems Physics, Henan University, Kaifeng 475004, People's Republic of China*
[3]*Key Laboratory of Materials Physics, Institute of Solid State Physics, Chinese Academy of Sciences, Hefei 230031, People's Republic of China*

(Received 10 September 2007; revised manuscript received 26 February 2008; published 14 May 2008)

The geometries, stabilities, electronic, and magnetic properties of the transition metal encapsulated $M\mathrm{Si}_n$ (M=Sc, Ti, V, Cr, Mn, Fe, Co, Ni, Cu, Zn; n=8–16) clusters have been systematically investigated by using density functional theory with generalized gradient approximation. It is shown that every transition metal atom (TMA) will fall into the center of Si outer frame and form a metal-encapsulated Si cage at a certain size (ScSi_{14}, TiSi_{12}, VSi_{12}, CrSi_{12}, MnSi_{11}, FeSi_{10}, CoSi_{10}, NiSi_{10} CuSi_{12}, and ZnSi_{14}). The size of the smallest cagelike structures cannot be determined by the radius of the TMA alone; the bonding properties and the orbital hybridization between TMA and Si atoms also play an important role. The stability of the cagelike $M\mathrm{Si}_n$ clusters cannot be understood by electron shell filling (18 or 20 electrons) rule; it depends on other factors. The total magnetic moments of $M\mathrm{Si}_n$ clusters and the magnetic moments of TMA in $M\mathrm{Si}_n$ clusters are not always quenched when the TMA falls into the center of the Si outer frame.

DOI: 10.1103/PhysRevB.77.195417 PACS number(s): 61.46.Bc, 36.40.Cg, 36.40.Mr

I. INTRODUCTION

Since the discovery of C_{60}, the cage cluster has been attracting a vast range of interest because of its structural completeness as a building unit of nanoscale materials and structures.[1] The cage structure also has the advantage that its hollow structure allows additional atoms to be contained in the cluster, thereby tailoring the properties. Motivated by the discovery and application of carbon fullerene,[2–4] people begin to think that is carbon the only element which can form fullerenelike structure? Are there any other elements that can also form fullernelike structure?

Much attention is focused on the silicon element first. Because silicon is isovalent to the carbon atom in the Periodic Table and it is a key element in the microelectronics industry, several efforts[5–10] have been made in the aim of designing a silicon cluster with a fullerenelike cage structure or creating a one-dimensional Si structure such as nanotube.

However, all these results show that silicon atoms tend to bind themselves against generating fullerenelike cages due to their sp^3 nature. As a matter of fact, Si_n clusters (n up to 50) usually favor compact forms, which are completely different from fullerene cages.[11,12] In addition, the structure of a Si_{60} cluster in a fullerene cage is highly distorted.[13]

Instead, some people suggested that Si cage clusters should be synthesized by adding suitable foreign atoms to terminate dangling bonds of Si, which inherently arise in cage-like networks. Many types of elements were doped in silicon clusters for the aim of searching stabilized foreign atom doped silicon clusters, including nonmetal atoms (carbon,[14] boron,[15] nitrogen,[16] and hydrogen[17,18]), reactive metal [alkali,[19,20] Be,[21] and Al (Ref. 22)], and transition metal (TM) atoms. Many researches[23–26] focusing on the growth behavior of TM-doped silicon clusters show that the TM-encapsulated cagelike clusters are always the magic clusters in the $M\mathrm{Si}_n$ clusters as the number of Si atoms increases.

So in recent years, many researches have focused on the TM doped silicon cagelike clusters both experimentally[27–31] and theoretically.[32–39] In these reports, the TM atoms were found to be a good dopant to stabilize the cagelike $M\mathrm{Si}_n$ clusters because of their suitable atom size and d-band filling. There are also some interesting discussions on the geometries, charge properties, magnetic properties, and electronic counting rule for the TM-silicon cagelike clusters.

Although there are so many studies about cagelike $M\mathrm{Si}_n$ clusters, especially for 3d TM, there are still several essential open questions about the $M\mathrm{Si}_n$ cage clusters.

(1) Can every type of transition metal atom (TMA) in $M\mathrm{Si}_n$ clusters completely falls into the center of Si outer frame and form metal-encapsulated Si cage at a certain size?

(2) What is the size of the smallest cagelike structures in every $M\mathrm{Si}_n$ clusters? What factors is the size related to? Is there any counting rule that can explain the stability of all these cagelike structures?

(3) What are the charge properties of these smallest cagelike clusters? Are the magnetic moments always quenched when the cagelike structure formed?

As an effort to address the above questions, here we provide an *ab initio* structural and electronic investigation for 3d transition metal doped silicon $M\mathrm{Si}_n$ (M=Sc, Ti, V, Cr, Mn, Fe, Co, Ni, Cu, Zn) clusters.

II. COMPUTATIONAL DETAILS

All theoretical computations were performed with a DMOL^3 package.[40,41] During the density-functional calculations, all electron treatment and double numerical basis including d-polarization function[40] were chosen. The exchange-correlation interaction was treated within the gen-

TABLE I. Calculated bond distance d (Å), vibrational frequency ω_e (cm^{-1}), experimental results, and previous theoretical study.

	Our results		Expt.		Theor.[a]	
Dimers	d	ω_e	d	ω_e	d	ω_e
ScSi	2.452	373			2.519	348
TiSi	2.474	352			2.447	359
VSi	2.331	348			2.379	323
CrSi	2.361	306			2.425	294
MnSi	2.229	368			2.308	325
FeSi	2.162	371			2.170	382
CoSi	2.092	425			2.123	392
NiSi	2.043	475	2.032[b]	467[b]	2.015	500
CuSi	2.234	340	2.298[c]	330[c]	2.242	325
ZnSi	2.436	234			2.429	239

[a] Reference 61.
[b] Reference 62.
[c] Reference 63.

eralized gradient approximation (GGA) by using BLYP functional.[42,43] Self-consistent field calculations were done with a convergence criterion of 2×10^{-5} hartree on total energy.

One of the smallest clusters for which encapsulation of a metal atom could occur is a cube, so we started our search on TM-encapsulated clusters from $n=8$ onward. As reported in Ref. 33, the suitable $M@\mathrm{Si}_n$ building blocks of self-assembly materials vary in the range of $10\leqslant n\leqslant 16$, so we ended our search at $n=16$. In this paper, equilibrium geometries of pure Si_n ($n=7-17$) clusters were optimized first based on the previous calculation results.[12,44–46] For the low-lying isomers of $M\mathrm{Si}_n$, we searched them extensively by two ways: (1) considering all of the possible structures reported in the previous papers and (2) placing a TM atom at various adsorption or substitutional sites on the basis of optimized Si_n geometries, i.e., TM-capped, TM-substituted, TM-concaved patterns, and Si-capped pattern.

Harmonic vibrational frequencies were calculated for the promising stationary points from a direct structural optimization; if an imaginary vibrational mode was found, a relaxation along coordinates of imaginary vibrational mode was carried out until the true local minimum was actually obtained. Therefore, all isomers for each cluster are guaranteed as the local minima. In addition, for each isomer, the spin electronic configuration was considered at least 1, 3, and 5 for even-electron clusters (Ti, Cr, Fe, Ni, Zn) and 2, 4, and 6 for odd-electron clusters (Sc, V, Mn, Co, Cu). In the cases when the total energy decreases with the increase of spin, we consider enhancing higher spin state until the energy minimum with respect to S is reached.

In order to test the reliability of our calculations, we calculated MSi dimers; the results are summarized in Table I. As seen from Table I, our results are in good agreement with the experimental and previous theoretical data. Consequently, our methods are reliable and accurate enough to be applied to describe the properties of $M\mathrm{Si}_n$ clusters.

III. RESULTS AND DISCUSSIONS

Using the computational scheme that is described in Sec. II, the smallest TM encapsulated Si cagelike clusters for $M\mathrm{Si}_n$ ($M=$Sc-Zn) are shown in Fig. 1. The ground-state structures and the binding per atom of pure Si_n ($n=9-15$) are also plotted in Fig. 1 for the purpose of comparison. The average binding energies $[E_b(n)]$, embedding energies (EEs), the highest occupied molecular orbital and lowest unoccupied molecular orbital (HOMO-LUMO) gaps, the vertical ionization potentials (VIPs), atomic charges, and magnetic

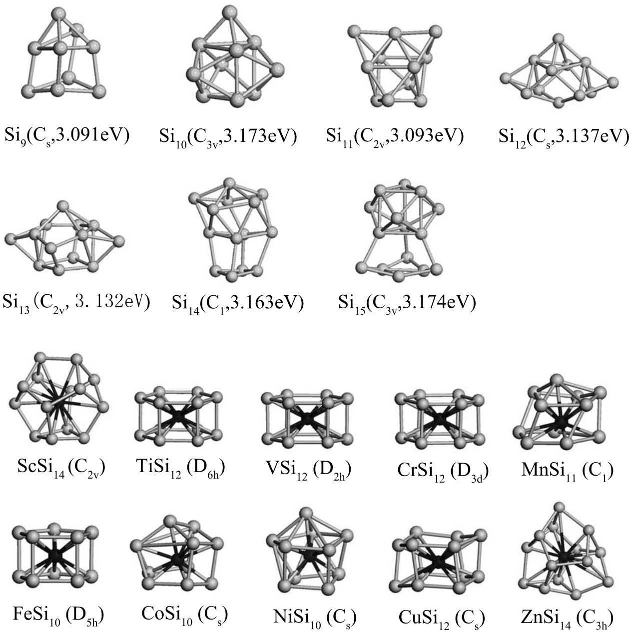

Si_9(C_s,3.091eV) Si_{10}(C_{3v},3.173eV) Si_{11}(C_{2v},3.093eV) Si_{12}(C_s,3.137eV)

Si_{13} (C_{2v}, 3. 132eV) Si_{14}(C_1,3.163eV) Si_{15}(C_{3v},3.174eV)

ScSi_{14} (C_{2v}) TiSi_{12} (D_{6h}) VSi_{12} (D_{2h}) CrSi_{12} (D_{3d}) MnSi_{11} (C_1)

FeSi_{10} (D_{5h}) CoSi_{10} (C_s) NiSi_{10} (C_s) CuSi_{12} (C_s) ZnSi_{14} (C_{3h})

FIG. 1. Groud-state stuctures of pure Si_n ($n=9-15$) clusters and structures of the smallest TM encapsulated Si cagelike clusters for $M\mathrm{Si}_n$ ($M=\mathrm{Sc},\mathrm{Ti},\mathrm{V},\mathrm{Cr},\mathrm{Mn},\mathrm{Fe},\mathrm{Co},\mathrm{Ni},\mathrm{Cu},\mathrm{Zn}$). Dark ball: transition metal atoms and light ball: silicon atoms.

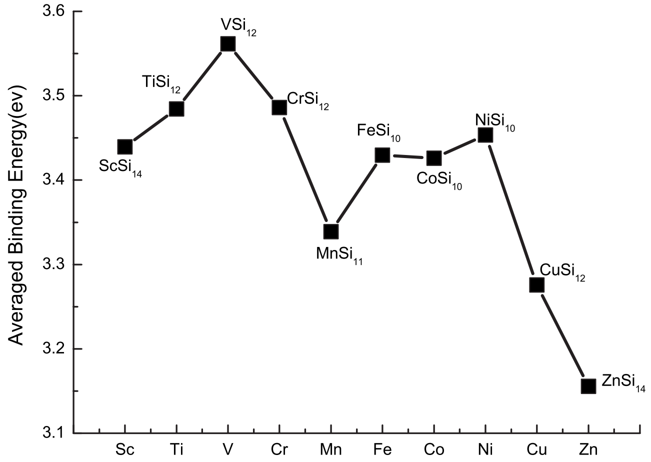

FIG. 2. The average binding energies of the smallest cagelike $M\mathrm{Si}_n$ ($M=\mathrm{Sc,Ti,V,Cr,Mn,Fe,Co,Ni,Cu,Zn}$) clusters.

moments of the smallest cagelike $M\mathrm{Si}_n$ clusters are shown in Figs. 2–4, and Fig. 5, respectively.

A. Structures of clusters

ScSi_{14} *and* ZnSi_{14}. The smallest Sc and Zn centered silicon cagelike clusters are reported here. Both of their ground-state structures can be seen as a fullerenelike cage, which consists of six pentagonal faces and three rhombii, but with different symmetries, C_{2v} for ScSi_{14} and C_{3h} for ZnSi_{14}. They have the lowest spin multiplicity (2, 1). While Reveles and Khanna[36] have an *ab initio* search of the ground state of ScSi_n ($n=15,16,17$) clusters and the structures they obtained are all cagelike structures with Sc atom in the center of the Si outer frame, the ground-state structure of ScSi_{15} can be seen as a Si atom bottom capped on the ScSi_{14} (Fig. 1) structure we obtained. In addition, Zdetis[38] studied $M\mathrm{Si}_n$ ($M=\mathrm{Zn,Cu,Ni}$) clusters with the framework of DFT, a hexagonal chair structure of C_{3v} symmetry is obtained as the ground state structure of ZnSi_{12}, whereas the hexagonal structure is only a low-lying isomer of ZnSi_{12} in our study, and a Zn on the vertex structure is the ground state structure, which is 0.280 eV lower in energy than that of the hexagonal structure.

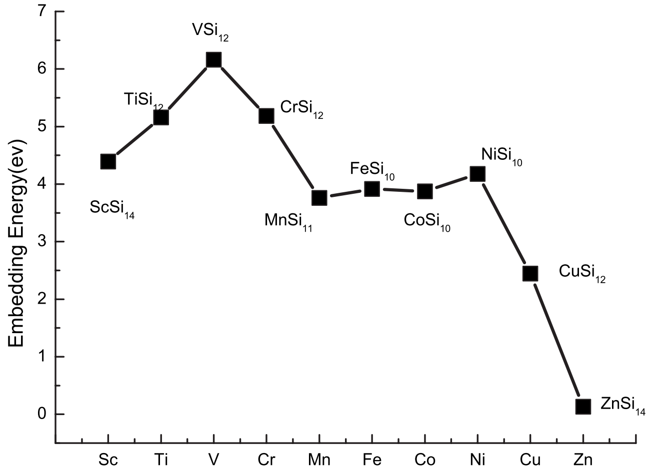

FIG. 3. The embedding energies of the smallest cagelike $M\mathrm{Si}_n$ ($M=\mathrm{Sc,Ti,V,Cr,Mn,Fe,Co,Ni,Cu,Zn}$) clusters.

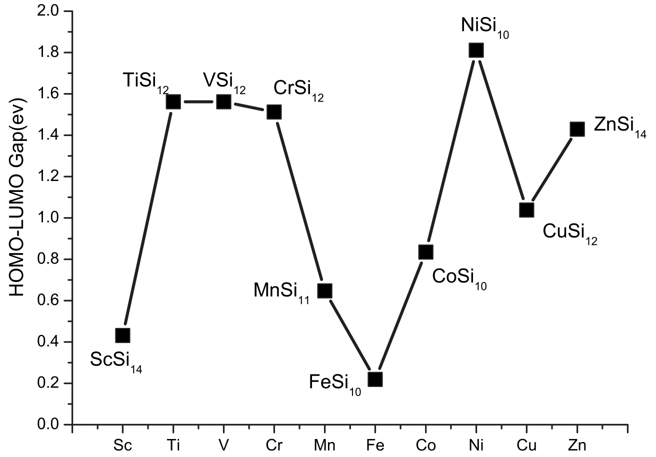

FIG. 4. The HOMO-LUMO gaps of the smallest cagelike $M\mathrm{Si}_n$ ($M=\mathrm{Sc,Ti,V,Cr,Mn,Fe,Co,Ni,Cu,Zn}$) clusters.

TiSi_{12}, VSi_{12}, CrSi_{12}, *and* CuSi_{12}. Starting from the same size $n=12$, each atom of Ti, V, Cr, and Cu in $M\mathrm{Si}_{12}$ clusters completely falls into the center of the Si frame and form a cage. The ground-state structures of them are all hexagonal prisms.

The hexagonal cage in case of Ti is a perfect cage (D_{6h}) with spin triplet, which is well consistent with Ref. 34. Nevertheless, the energy of the singlet state is only 0.025 eV higher than that of the ground state, but with only C_1 symmetry. In Ref. 47, the growth behavior of $M\mathrm{Si}_n$ ($M=\mathrm{Ti}$, Zr, Hf; $n=8-16$) clusters was studied by using an *ab initio* ultrasoft pseudopotential plane wave method. They found that for $n=8-12$, the basketlike open structures were the most favorable, while for $n=13-16$, the metal atom was completely surrounded by silicon atoms, whereas our study suggests that the TiSi_n clusters adopt cagelike structure with Ti atom encapsulated in the interior site when $n=12$, which is consistent with the latest calculational results.[23] The hexagonal cage in the cases of VSi_{12} (D_{2h}) and CrSi_{12} (D_{3d}) well

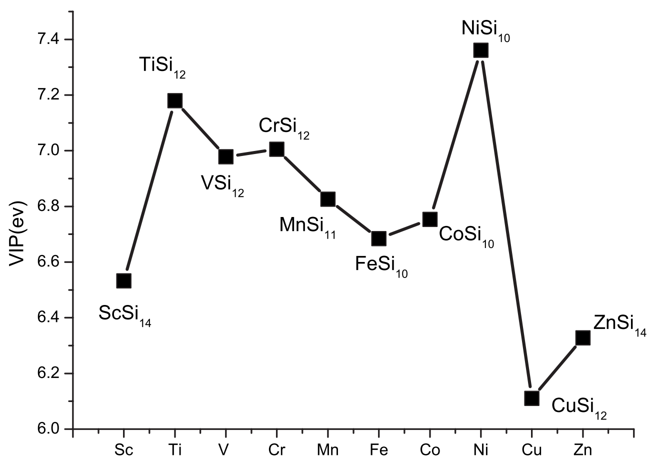

FIG. 5. The VIP of the smallest cagelike $M\mathrm{Si}_n$ ($M=\mathrm{Sc,Ti,V,Cr,Mn,Fe,Co,Ni,Cu,Zn}$) clusters.

TABLE II. The size of the smallest cage of $M\mathrm{Si}_n$ (M=Sc, Ti, V, Cr, Mn, Fe, Co, Ni, Cu, Zn) clusters and the radius of the TM atom.

Clusters	ScSi_n	TiSi_n	VSi_n	CrSi_n	MnSi_n	FeSi_n	CoSi_n	NiSi_n	CuSi_n	ZnSi_n
Size	14	12	12	12	11	10	10	10	12	14
AR (pm)	164.1	144.8	132.1	124.9	136.6	124.1	125.3	124.6	127.8	133.2

consists with the previous results.[23,48,49] For CuSi_{12}, the hexagonal prism is more distorted than the other three prisms, with C_s symmetry only, which is well consistent with the results that are obtained in Ref. [39,50].

FeSi_{10}, CoSi_{10}, *and* NiSi_{10}. Fe, Co, or Ni atom falls into the center of the Si frame and forms the smallest cagelike structure at the size of $n=10$. Different from Ti, V, or Cr, in which the smallest cagelike structures are all with hexagonal symmetry, the ground-state structures of FeSi_{10}, CoSi_{10}, and NiSi_{10} have the following characteristics. For FeSi_{10} cluster, the ground-state structure is a perfect Fe centered pentagonal prism (D_{5h}) with spin triplet. In fact, Ma *et al.*,[25] Mpourmpakis *et al.*,[26] and Lu and Nagase[33] also obtained a pentagonal prism as the ground state structure for FeSi_{10} cluster, whereas the lowest-energy structures of CoSi_{10} and NiSi_{10} are both constructed in the base of a two-layer Si cage with a trapezia and a pentagon on each layer and one additional Si atom on the bottom.

For CoSi_n, it was found that a Co centered distorted cube (C_s) with one Si atom capped on the bottom as the smallest CoSi_n cagelike cluster when $n=9$.[51] However, the latest report[52] also by this group says that the lowest-energy structures of CoSi_9 and CoSi_{10} have different geometries, in which CoSi_9 is neither the magic nor the smallest cagelike structure. Instead, CoSi_n clusters adopt cagelike structures with Co atom encapsulated inside when $n\geqslant 10$. Our results support this conclusion. Additionally, we have searched a new lowest–energy lying CoSi_{10} structure (Fig. 1), which can be seen as a two-layer Si cage with a trapezia and a pentagon on each layer and one additional Si atom on the trapezia.

For NiSi_{10}, similar as the ground state structure of CoSi_{10}, we obtained a two-layer Si cage with a trapezia and a pentagon on each layer and one additional Si atom on the pentagon. A Ni centered distorted cube (C_s) was obtained as the smallest cagelike structure at the size of $n=8$.[53] However, in our calculations, this structure does not exist after geometry optimization. Most recently, an extensive search for the lowest-energy structure of NiSi_n ($n=1-14$) clusters with in all-electron DFT was reported,[54] and the same ground-state structure when $n=9$, 10 was obtained as we did. However, we do not agree with that NiSi_9 is a cagelike structure: it should be defined as a basketlike structure because the Ni atom is very close to the surface.[47,48] So, we believe that NiSi_{10} is indeed the smallest cagelike cluster in NiSi_n clusters.

MnSi_{11}. The smallest Mn doped silicon cagelike structure is found at the size of $n=11$. It can be viewed as a Mn centered distorted pentagonal prism (C_1) with one Si atom capped on the top.

As shown in Fig. 1, it can be seen that every TMA in 3*d* series can fall into the center of Si outer frame in $M\mathrm{Si}_n$ clusters and form the metal-encapsulated Si cage at a certain size. The size of the smallest cage is shown in Table II.

In previous papers,[25,47] the reason why cagelike structure began to be formed at different critical sizes was always understood by the radius of the metal atom. The bigger the TM atom was, the more Si atoms were needed to completely; encapsulate the TMA the size of the smallest cagelike structure depended on the size of metal atom and the number of Si atoms, whereas in our study, as shown in Table II, it can be found that there is no corresponding relationship between the radius of the TMA and the size in which a cagelike structure formed. The radii of Ti, V, and Cr are apparently different, but they form the smallest cagelike structure at the same size $n=12$. Fe, Co, and Ni have the similar radii and form the smallest cagelike structure at the same size $n=10$, but the ground-state structures of FeSi_{10}, CoSi_{10}, and NiSi_{10} are very different.

Zn atom has the relatively small radius in 3*d* series, but the size of its smallest cagelike structure is the largest. The radius of Cu atom is similar to that of Fe, Co, and Ni, but it forms the cagelike structure at the size $n=12$, which is the same as Ti, V, and Cr. Both Zn and Cu atoms have filled all *d* shells, the bonding in $\mathrm{Cu@Si}_{12}$ should have a significant ionic component, while Zn is a closed shell system; the bonding in $\mathrm{Zn@Si}_{14}$ should have a van der Waals component. However, for Sc, Ti, V, Cr, Mn, Fe, Co, and Ni, the bonding is dominated by the *d* electrons in various types of *pd* hybridization.

So, we can conclude from the above discussions that the reason why the $M\mathrm{Si}_n$ clusters form a cagelike structure at different sizes cannot be explained only by the radius of the TM atoms, the bonding properties, and the orbital hybridization between the TMA and Si atoms that also play an important role.

B. Stability and counting rule

It is well known that the relative stability of the clusters can be predicted by calculating the average binding energies $[E_b(n)]$, the EEs, the VIPs, and HOMO-LUMO gaps.

The average binding energies $[E_b(n)]$, EEs, and VIP for the $M\mathrm{Si}_n$ clusters can be defined as the following formulas:

$$E_b(n) = [E_T(M) + nE_T(\mathrm{Si}) - E_T(M\mathrm{Si}_n)]/n + 1, \tag{1}$$

$$\mathrm{EE} = E_T(M) + E_T(\mathrm{Si}_n) - E_T(M\mathrm{Si}_n), \tag{2}$$

$$\mathrm{VIP} = E_T(M\mathrm{Si}_n^+) - E_T(M\mathrm{Si}_n), \tag{3}$$

where $E_T(M\mathrm{Si}_n)$, $E_T(\mathrm{Si})$, $E_T(M)$, $E_T(\mathrm{Si}_n)$, and $E_T(M\mathrm{Si}_n^+)$ represent the total energies of the most stable $M\mathrm{Si}_n$, Si, M, Si_n, and $M\mathrm{Si}_n^+$ clusters, respectively.

The calculated results of $M\mathrm{Si}_n$ clusters on the average binding energies $[E_b(n)]$, the EEs, the VIPs, and HOMO-

TABLE III. The charge, total magnetic moments (TMMs), magnetic moments of TM atom (MMTM), Mulliken population (MP), and magnetic moments of 3*d*, 4*s*, and 4*p* states for transition metal atom in the smallest cagelike $M\mathrm{Si}_n$ (M=Sc, Ti, V, Cr, Mn, Fe, Co, Ni, Cu, Zn) clusters.

				3*d*		4*s*		4*p*	
	Charge	MMTM	TMM	MP	Moments	MP	Moments	MP	Moments
ScSi_{14}	−0.503	0.318	1.000	2.359	0.293	0.593	0.008	0.527	0.017
TiSi_{12}	−0.522	0.782	1.999	3.254	0.703	0.620	0.019	0.633	0.060
VSi_{12}	−0.567	0.384	1.001	4.233	0.357	0.645	0.010	0.677	0.018
CrSi_{12}	−0.858	0.000	0.000	5.378	0.000	0.648	0.000	0.836	0.000
MnSi_{11}	−0.679	1.103	0.998	6.306	1.059	0.687	0.014	0.678	0.031
FeSi_{10}	−0.610	1.096	2.000	7.131	1.077	0.763	−0.001	0.706	0.021
CoSi_{10}	−0.815	0.191	1.000	8.233	0.170	0.783	0.000	0.792	0.022
NiSi_{10}	−0.690	0.000	0.000	8.793	0.000	0.946	0.000	0.000	0.000
CuSi_{12}	−0.538	0.029	0.099	9.787	0.048	0.882	−0.006	0.875	−0.015
ZnSi_{14}	−0.284	0.000	0.000	9.919	0.000	1.188	0.000	1.177	0.000

LUMO gaps are shown in Figs. 2–5, respectively.

According to the 18-electron rule[55] the most stable $M\mathrm{Si}_{12}$ clusters should be CrSi_{12}, and the most stable $M\mathrm{Si}_{10}$ clusters should be FeSi_{10}. However, the results that are shown in Figs. 2–5 indicate that CrSi_{12} and FeSi_{10} do not have the highest $E_b(n)$, EE, VIP, and HOMO-LUMO gaps. It is the highest for VSi_{12} and NiSi_{10} as opposed to CrSi_{12} and FeSi_{10}. Assuming that each Si contributes one valence electron, VSi_{12} and NiSi_{10} would contain 17 and 20 electrons, respectively. So, we can conclude from the above four figures that the 18-electron rule has a limited applicability in $M\mathrm{Si}_n$ clusters, and our results are consistent with the discussion in Refs. 34 and 23.

However, somebody hold the different opinions in their recent works,[35–37] and they insist that the embedding energy calculated via the Eq. (2) ignoring the Wigner–Witmer (WW) rule.[56] The WW rule requires that the products reaction have the same spin multiplicity as reactants. One should therefore calculate EE that is defined by

$$\mathrm{EE}^{W\text{-}W} = E_T^{M_s}(M) + E_T(\mathrm{Si}_n) - E_T^{M_s}(M\mathrm{Si}_n), \tag{4}$$

where the energy of the transition metal atom should be calculated by considering the same spin multiplicity M_s as for the $M\mathrm{Si}_{12}$ clusters. Applying such rule in Ref. 35, CrSi_{12} and FeSi_{12} were found to exhibit the highest binding energy across the neutral, while VSi_{12}^- had the highest binding energy across the anionic $M\mathrm{Si}_{12}$ series. However, in their calculations, when they calculated in Eq. (4), the octet rule is valid in neutral clusters, the maximum at 20 electrons (MnSi_{12}^-) is not marked, and CoSi_{12}^- cluster which has 22 electrons exhibits special stability. Namely, no matter how it is calculated in each equation, the octet rule is not a perfect rule. In addition, as reported in Ref. 37, the stability at 18 and 20 electrons holds for M=5*d* transition metal both with the Wigner–Wimer and Hund's rule.

Wigner–Witmer rule is originally derived from group theory, it is always used to predict the possible electronic states of diatomic molecules (HCl, CO, etc.) from the given electronic states of separated atoms. However, its reliability needs to be discussed.

An 18-electron rule was first used in inorganic chemistry and organometallic chemistry of TM atoms and was only an empirical rule, which was obtained by summarizing from many experimental results. Although it actually recapitulate many experiment, there are many exceptional cases, such as TiF_6^+, $\mathrm{V(CO)}_6$, and $\mathrm{Co(C_2H_5)}_2$, whose coordination electron numbers are equal to 16, 17, and 21.

Fundamentally speaking, every theory should be able to well explain the experimental results. However, in a few experimental results, it can be found that many clusters do not obey the counting rule. For example, Beck[57] produced $M@\mathrm{Si}_{15}^+$ and $M@\mathrm{Si}_{16}^+$ clusters with M=Mo, and W. Ohara *et al.*[29] produced $M@\mathrm{Si}_n^-$ clusters, which n=15 and 16 were found to be the most stable for M=Ti, Mo, Hf, and W. Jaeger *et al.*[31] found that chromium-silicon clusters in the higher mass range have more in tense peaks at $\mathrm{Cr}@\mathrm{Si}_{15}^+$ and $\mathrm{Cr}@\mathrm{Si}_{16}^+$ masses. Although WSi_{12} cluster which abides by 18-electron rule was produced by Hiura *et al.*[27] in an ion trap and confirmed to be a W-encapsulating Si_{12} cage cluster with higher relative stability, both the results that are calculated in Eq. (4) (Ref. 37) and Eq. (2) (Ref. 34) showed that WSi_{12} was the most stable among the $M\mathrm{Si}_{12}$ clusters.

To sum up, it is shown that electron shell filling rule (18- or 20-electron rule) is just one of the aspects which determine the stability of clusters. A possible explanation of the limited applicability of the 18-electron rule is that the stability depends on other factors, such as the size of the metal atom, *pd* hybridization, and *d* state shell of TMA. An 18-electron rule is just a rule, not a law.

C. Charge transfer and magnetic moments

We have performed Mulliken population analysis for the lowest-energy structures. The atomic charge of TM atom in cagelike structures $M\mathrm{Si}_n$ clusters are listed in Table III and plotted in Fig. 6. As seen from Fig. 6, charge always transfers from Si atoms to TM atom, indicating that TMA acts as

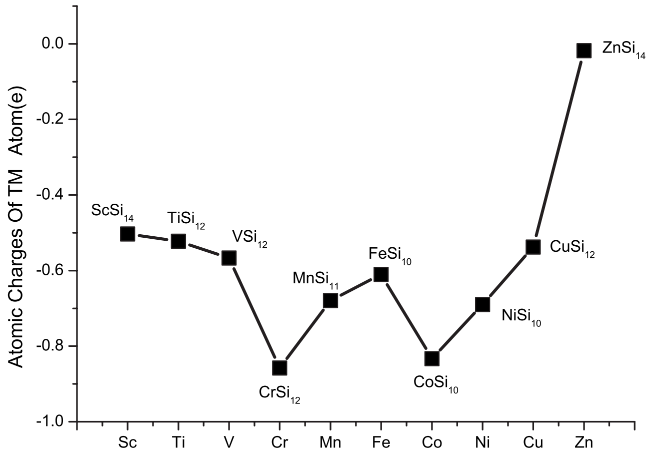

FIG. 6. Atomic charges of TM atom of the smallest cagelike $M\mathrm{Si}_n$ ($M=\mathrm{Sc,Ti,V,Cr,Mn,Fe,Co,Ni,Cu,Zn}$) clusters.

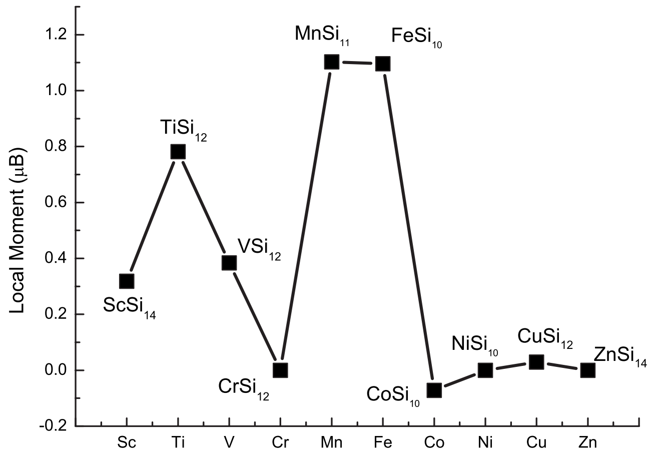

FIG. 8. Magnetic moments of TM atom of the smallest cagelike $M\mathrm{Si}_n$ ($M=\mathrm{Sc,Ti,V,Cr,Mn,Fe,Co,Ni,Cu,Zn}$) clusters.

an electron acceptor in the smallest $M\mathrm{Si}_n$ cagelike structures. Zn in ZnSi_{14} has apparently less charge transfer with Si atoms because of its close shelling.

Based on the optimized geometries, the magnetic properties of $M\mathrm{Si}_n$ clusters were computed and results are presented in Table III and plotted in Figs. 7 and 8.

As shown in Table III and Figs. 7 Fig. 8, it can be found that the total magnetic moments of the $M\mathrm{Si}_n$ clusters and the magnetic moments on TMA are not always quenched when the TMA encapsulated in Si outer frame cage but have an oscillation. The magnetic moments of CrSi_{12}, NiSi_{10}, and ZnSi_{14} clusters and the TM in them are completely quenched. For MnSi_{11} and FeSi_{10}, the total magnetic moments are mainly located on the Mn and Fe atom, some of the local moments on Si atoms are found to align antiferromagnetic with respect to that on Mn and Fe atoms. For ScSi_{14}, TiSi_{12}, VSi_{12}, CuSi_{12}, and CoSi_{10}, the total magnetic moments contributed by TM atoms are small.

A detailed analysis of the one-site atomic charges and local magnetic moments was performed to further understand the charge transfer and the magnetic properties of $M\mathrm{Si}_n$ cagelike clusters. As shown in Table III, the magnetic moments of TMA are mainly from the $3d$ state, following this is the $4s$ state, and the $4p$ state contributes little to the magnetic moments of TMA. The $3s$ and $3p$ states of Si also have made a contribution to the total magnetic moments of the $M\mathrm{Si}_n$ clusters. In the case of $M\mathrm{Si}_n$ (M=Sc-Ni), the $3d$ state obtains some amount of electrons and $4s$ state loses some electrons. However, for Cu and Zn, both the $3d$ and $4s$ states tend to lose a very few amount of electrons. Namely, there is internal electron transfer among $3d$, $4s$, and $4p$ states in TM atom. Thus, for the $M\mathrm{Si}_n$ clusters, the charge transfer mainly happens between TM $4s$, $3d$, $4p$ and Si $3s$, $3p$ states. So, there exist *sdp* hybridization in TMA and *s-p* hybridization in Si atom, and there also exist hybridization between TMA and Si atoms.

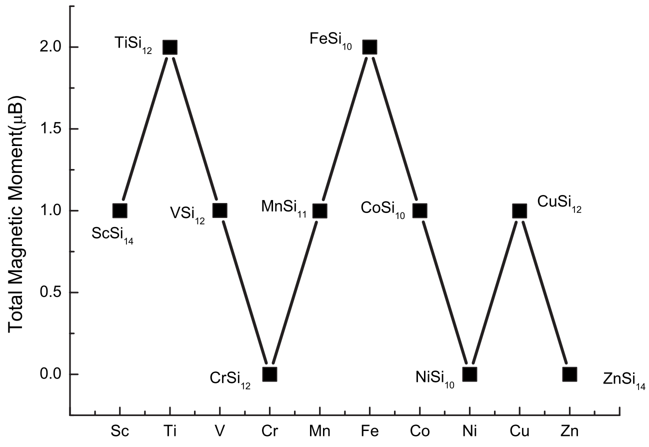

FIG. 7. Total magnetic moments of the smallest cagelike $M\mathrm{Si}_n$ ($M=\mathrm{Sc,Ti,V,Cr,Mn,Fe,Co,Ni,Cu,Zn}$) clusters.

Magnetic properties are one of the most interesting in physics. In cluster size, there are even more different properties from molecular or bulk materials. Many efforts have been made to explain the quenching of magnetic moments.

Ma *et al.*[25] conjectured that there might be some correlation between geometry structure of Si framework and the magnetic moments of the encapsulated Fe atom. The charge transfer and the strong hybridization between Fe $4s$, $3s$ and Si $3s$, $3p$ states may be one major reason for quenching the magnetic moments of Fe atom. Khanna *et al.*[48] reported, in the case of CrSi_{12} cluster, the magnetic moments of Cr was completely quenched. They believed that this result was from strong hybridization between Cr $3d$ and $3s$, $3p$ states of Si. Rao and Jena[58] found that the quenching of the Ni_n moments in Ni_n $(\mathrm{benzene})_m$ arises due to the strong hybridization between the $3d$ electrons of nickel and the π electrons of benzene. In a combined experimental and theoretical study, Janssens *et al.*[59] considered the intermediate bimetallic clusters composed of silver (Ag) and the $3d$ transition metal (M=Sc-Ni) and presented the first example of magnetic-element-doped metal clusters, which showed quenching of the impurity magnetic moments for selected sizes. They reported that with the delicate energy balance between Hund's rule and electronic shell closing, the quenching of magnetic moments at the impurity was likely induced by the gain in energy related with the 18-electron shell closing.

Pandey *et al.*[60] found that when TMAs were supported on benzene, the magnetic moments for Sc, Ti, and V were enhanced by $2\mu_B$, while for Mn, Fe, Co, and Ni, they were reduced by 2 μ_B from their free atom value. The magnetic moments of Cr remained unchanged. They explained that this variation was the direct consequence of Pauli exclusion principle and was rooted in the chemistry of the transition metal atoms. This behavior could be simply understood by considering the Pauli exclusion principle and the chemistry of the transition metal atoms as well as that of benzene.

However, none of these above conjunctions can well explain $M\mathrm{Si}_n$ clusters. For CrSi_n and NiSi_n clusters, the magnetic moments of them begin to be quenched at the smallest size ($n=8$) we studied, not only be quenched at the size ($n=12$ and $n=10$) when the cagelike structure formed. The magnetic properties of FeSi_n clusters are even more special, in which the magnetic moments of FeSi_n are quenched at the size of $n=9$ but emerged at $n=10$ and 11, then quenched again when $n \geqslant 12$, whereas other $M\mathrm{Si}_n$ clusters do not have this phenomenon. To sum up, the quenching of magnetic moments in $M\mathrm{Si}_n$ clusters cannot be explained only by close shell, *pd* hybridization, geometry, symmetry, Si encapsulated, Hund's rule, or Pauli exclusion principle. A more advanced theory is needed to explain this phenomenon, and the studies are currently in progress.

IV. CONCLUSIONS

By using first-principles DFT-GGA calculations, the geometries, stabilities, and magnetic properties of the TM encapsulated $M\mathrm{Si}_n$ ($M=$Sc, Ti, V, Cr, Mn, Fe, Co, Ni, Cu, Zn; $n=8-16$) clusters have been systematically studied. The results are summarized as follows.

(1) Every TMA will fall into the center of Si outer frame and form a metal-encapsulated Si cage at a certain size (ScSi_{14}, TiSi_{12}, VSi_{12}, CrSi_{12}, MnSi_{11}, FeSi_{10}, CoSi_{10}, CuSi_{12}, and ZnSi_{14}). The size of the smallest cagelike structures is not determined by the radius of the TMA, the bonding properties, and the orbital hybridization between TMA and Si atoms which also perform an important role.

(2) The electron shell filling (18- or 20-electron rule) rule has a limited applicability since we found that stability depends on other factors as well (*d* state shell of TMA, *pd* hybridization, the atom size, etc.).

(3) The charge in the smallest $M\mathrm{Si}_n$ cagelike clusters always transfers from Si atoms to the TMA; there is also internal electron transfer among 3*d*, 4*s*, and 4*p* states in TMA.

(4) The total magnetic moments of $M\mathrm{Si}_n$ clusters and the magnetic moments of TMA in $M\mathrm{Si}_n$ clusters are not always quenched when the TMA falls into the center of the Si outer frame. The magnetic moments of CrSi_{12}, NiSi_{10}, and ZnSi_{14} are completely quenched. The total magnetic moments are not only contributed by TMA but also by Si atoms. The reason why the magnetic moments are quenched for certain TMA at certain sizes is still an uncertain question.

Note added in proof. In Ref. 64, Reis *et al.* are also interested in cagelike transition metal doped silicon clusters. They investigated the main structural and electronic properties of the $\mathrm{Ti@Si}_{16}$ molecular solid by using density-functional theory. In our work, we focus on the smallest isolated cagelike clusters and their properties. As reported in our work, $\mathrm{Ti@Si}_n$ clusters begin to form a Ti centered cagelike structure at the size of $n=12$. The size of the $\mathrm{Ti@Si}_{16}$ cluster is larger than 12, which is consistent with our prediction. In addition, Reis *et al.* investigated bulk forms of cagelike cluster assembled material. In our further work, we will also construct a Si nanotube by using $M@\mathrm{Si}_{12}$ hexagonal prism or $M@\mathrm{Si}_{10}$ pentagonal prism as the basic unit.

ACKNOWLEDGMENTS

This work was supported by the National Science Foundation of China under Grants No. 10504036 and No. 90503005, by the special Funds for Major State Basic Research Project of China (973) under Grant No. 2005CB623603, by the Henan University National Science Foundation under Grant No. 06YBZR021, by Knowledge Innovation Program of Chinese Academy of Sciences, and by Director Grants of Hefei Institutes of Physical Sciences. Part of the calculations were performed at the Center for Computational Science, Hefei Institutes of Physical Sciences.

---

*Author to whom correspondence should be addressed. zgf@henu.edu.cn

[1] R. E. Smalley and B. I. Yakobson, Solid State Commun. **107**, 597 (1998).

[2] H. W. Kroto, J. R. Heath, S. C. O'Brien, R. F. Curl, and R. E. Smalley, Nature (London) **318**, 162 (1985).

[3] S. Iijima, Nature (London) **354**, 56 (1991).

[4] W. Kratschmer, L. D. Lamb, K. Fostiropoulos, and D. R. Huffman, Nature (London) **347**, 354 (1990).

[5] M. Harada, S. Osawa, E. Osawa, and E. D. Jemmis, Chem. Phys. Lett. **1**, 1037 (1994).

[6] E. D. Jemmis, J. Leszczynski, and E. Osawa, Fullerene Sci. Technol. **6**, 271 (1998).

[7] E. F. Sheka, E. A. Nikitina, V. A. Zayets, and I. Y. Ginzburg, Int. J. Quantum Chem. **88**, 441 (2002).

[8] H. Tanaka, S. Osawa, J. Onoe, and K. Takeuchi, J. Phys. Chem. B **103**, 5939 (1999).

[9] X. G. Gong and Q. Q. Zheng, Phys. Rev. B **52**, 4756 (1995).

[10] Q. Sun, Q. Wang, P. Jena, B. K. Rao, and Y. Kawazoe, Phys. Rev. Lett. **90**, 135503 (2003).

[11] E. C. Honea, A. Ogura, C. A. Murray, Krishnan Raghavachari, W. O. Sprenger, M. F. Jarrold, and W. L. Brown, Nature (London) **366**, 42 (1993).

[12] K. M. Ho, A. A. Shvartsburg, B. Pan, Z. Y. Lu, C. Z. Wang, J. G. Wacker, J. L. Fye, and M. F. Jarrold, Nature (London) **392**, 582 (1998).

[13] B. X. Li, P. L. Cao, and D. L. Que, Phys. Rev. B **61**, 1685 (2000).

[14] M. N. Huda and A. K. Ray, Phys. Rev. A **69**, 011201(R) (2004).

[15] C. Majumder and S. K. Kulshreshtha, Phys. Rev. B **70**, 245426 (2004).

[16] G. Jungnickel, T. Frauenheim, and K. A. Jackson, J. Chem. Phys. **112**, 1295 (2000).

[17] G. Belomion, J. Therrien, A. Smith, S. Rao, R. Twesten, S. Chaieb, M. H. Nayfeh, L. Wagner, and L. Mitas, Appl. Phys. Lett. **80**, 841 (2002).

[18] V. Kumar and Y. Kawazoe, Phys. Rev. Lett. **90**, 055502 (2003).

[19] C. Sporea, F. Rabilloud, and M. Aubert-Frecon, J. Mol. Struct.: THEOCHEM **802**, 85 (2007).

[20] S. Wei, R. N. Barnett, and U. Landman, Phys. Rev. B **55**, 7935 (1997).

[21] A. K. Singh, V. Kumar, T. M. Brieve, and Y. Kawazoe, Nano Lett. **2**, 1243 (2002).

[22] S. C. Zhan, B. X. Li, and J. S. Yang, Physica B **387**, 421 (2007).

[23] G. K. Gueorguiev, J. M. Pacheco, S. Stafstrom, and L. Hultman, Thin Solid Films **515**, 1192 (2006).

[24] J. Wang and J. G. Han, J. Chem. Phys. **123**, 064306 (2005).

[25] L. Ma, J. J. Zhao, J. G. Wang, B. L. Wang, Q. L. Lu, and G. H. Wang, Phys. Rev. B **73**, 125439 (2006).

[26] G. Mprourmparkis, G. E. Froudakis, A. N. Andriotis, and M. Menon, J. Chem. Phys. **119**, 7498 (2003).

[27] H. Hiura, T. Miyazaki, and T. Kanayama, Phys. Rev. Lett. **86**, 1733 (2001).

[28] M. Ohara, K. Miyajima, A. Pramann, A. Nakajima, and K. Kaya, J. Phys. Chem. A **106**, 3702 (2002).

[29] M. Ohara, K. Koyasu, A. Nakajima, and K. Kaya, Chem. Phys. Lett. **371**, 490 (2003).

[30] K. Koyasu, M. Akutsu, M. Mitsui, and A. Nakajima, J. Am. Chem. Soc. **127**, 4998 (2005).

[31] J. B. Jaeger, T. D. Jaeger, and M. A. Duncan, J. Phys. Chem. A **110**, 9310 (2006).

[32] T. Miyazaki, H. Hiura, and T. Kanayama, Phys. Rev. B **66**, 121403(R) (2002).

[33] J. Lu and S. Nagase, Phys. Rev. Lett. **90**, 115506 (2003).

[34] P. Sen and L. Mitas, Phys. Rev. B **68**, 155404 (2003).

[35] J. U. Reveles and S. N. Khanna, Phys. Rev. B **72**, 165413 (2005).

[36] J. U. Reveles and S. N. Khanna, Phys. Rev. B **74**, 035435 (2006).

[37] N. Uchida, T. Miyazaki, and T. Kanayama, Phys. Rev. B **74**, 205427 (2006).

[38] A. D. Zdetsis, Phys. Rev. B **75**, 085409 (2007).

[39] F. Hagelberg, C. Xiao, and W. A. Lester, Jr., Phys. Rev. B **67**, 035426 (2003).

[40] DMOL is a density-functional theory package distributed by MSI; B. Delley, J. Chem. Phys. **92**, 508 (1990).

[41] B. Delley, J. Chem. Phys. **113**, 7756 (2000).

[42] C. Lee, W. Yang, and R. G. Parr, Phys. Rev. B **37**, 785 (1988).

[43] A. D. Becke, J. Chem. Phys. **88**, 2547 (1988).

[44] L. M. Marim, M. R. Lemes, and A. Dal Pino, Jr., Phys. Rev. A **67**, 033203 (2003).

[45] A. A. Shvartsburg, B. Liu, M. F. Jarrold, and K. M. Ho, J. Chem. Phys. **112**, 4517 (2000).

[46] J. C. Yang, W. G. Xu, and W. S. Xiao, J. Mol. Struct.: THEOCHEM **719**, 89 (2005).

[47] H. Kawamura, V. Kumar, and Y. Kawazoe, Phys. Rev. B **71**, 075423 (2005).

[48] S. N. Khanna, B. K. Rao, and P. Jena, Phys. Rev. Lett. **89**, 016803 (2002).

[49] H. Kawamura, V. Kumar, and Y. Kawazoe, Phys. Rev. B **70**, 245433 (2004).

[50] C. Xiao, F. Hagelberg, and W. A. Lester, Jr., Phys. Rev. B **66**, 075425 (2002).

[51] L. Ma, J. J. Zhao, J. G. Wang, B. L. Wang, Q. L. Lu, and G. H. Wang, Chem. Phys. Lett. **411**, 279 (2005).

[52] J. G. Wang, J. J. Zhao, L. Ma, B. L. Wang, and G. H. Wang, Phys. Lett. A **367**, 335 (2007).

[53] Z. Y. Ren, F. Li, P. Guo, and J. G. Han, J. Mol. Struct.: THEOCHEM **718**, 165 (2005).

[54] J. Wang, Q. M. Ma, Z. Xie, Y. Liu, and Y. C. Li, Phys. Rev. B **76**, 035406 (2007).

[55] C. A. Tolman, Chem. Soc. Rev. **1**, 337 (1972).

[56] E. wigner, and E. E. Witmer, Z. Phys. **51**, 859 (1928).

[57] S. M. Beck, J. Chem. Phys. **90**, 6306 (1989).

[58] B. K. Rao and P. Jena, J. Chem. Phys. **116**, 1343 (2002).

[59] E. Janssens, S. Neukermans, H. M. T. Nguyen, M. T. Nguyen, and P. Lievens, Phys. Rev. Lett. **94**, 113401 (2005).

[60] R. Pandy, B. K. Rao, P. Jena, and J. M. Newsam, Chem. Phys. Lett. **321**, 142 (2000).

[61] Z. J. Wu and Z. M. Su, J. Chem. Phys. **124**, 184306 (2006).

[62] N. F. Lindholm, D. J. Burgh, G. K. Rothschopf, S. M. Sickafoose, and M. D. Morse, J. Chem. Phys. **118**, 2190 (2003).

[63] J. J. Scherer, J. B. Paul, C. P. Collier, and R. J. Saykally, J. Chem. Phys. **102**, 5190 (1995).

[64] C. L. Reis, J. L. Martins, and J. M. Pacheco, Phys. Rev. B **76**, 233406 (2007).